Solar Phys (2009) 255: 253–271
DOI 10.1007/s11207-009-9325-x

Polarization of Microwave Radio Emission of Flare-Producing Solar Active Regions

Vladimir M. Bogod · Leonid V. Yasnov

Received: 29 November 2007 / Accepted: 14 February 2009 / Published online: 12 March 2009

Abstract On the basis of our multiwavelength observations made with the one-dimensional RATAN-600 radio telescope, we study the inversion of the circular polarization in the solar microwave emission at different frequencies. The inversion is detected in the emission of flare-producing active regions (FPARs) at various stages of their development, starting from the pre-flare stage. During the latest 23rd solar cycle maximum, numerous FPARs revealed spectral inhomogeneities in their polarized microwave radiation (Bogod and Tokhchukova, 2003, *Astron. Lett.* **29**, 263). Here, we discuss a particular case of such inhomogeneities, the frequency-dependent double inversion of the sign of circular polarization, which probably reflects some essential processes in FPARs. We consider several mechanisms for the double inversion: linear interaction of waves in the region of a quasitransverse magnetic field, the propagation of waves through a region of zero magnetic field, the scattering of radio waves on waves of high-frequency plasma turbulence, the influence of the current fibrils on the propagation of the radio emission, and the magnetic "dips," in which the direction of magnetic field lines changes the sign relative to the observer. All of them have shortcomings, but the last mechanism explains the observations the best.

Keywords Sun · Flare · Solar active regions · Radio emission · Polarization · Pre-flare processes

1. Introduction

The sign inversion of circular polarization of the microwave radiation of radio sources on the Sun was discovered and studied by Piddington and Minnett (1951) and Peterova and Akhmedov (1974). The phenomenon was observed at centimeter wavelengths when active

V.M. Bogod (✉)
Special Astrophysical Observatory, St. Petersburg 196140, Russia
e-mail: vbog_spb@mail.ru

L.V. Yasnov
Radiophysics Research Institute of St. Petersburg State University, St. Petersburg 198504, Russia

regions (ARs) were passing across the disk of the Sun, for the polarization of the radio emission of the slowly varying component (SVC). Using low-resolution polarization data of the SVC, Peterova and Akhmedov (1974) found that in more than 50% of cases the sign of polarization reverses when an active region crosses the central meridian. This inversion was explained by the propagation of the radiation through the quasitransverse (QT) layer in the magnetic field (Cohen, 1960; Zheleznyakov, 1970; Bandiera, 1982). Such layers occur in regions where the angle between the magnetic field and the line of sight (the direction of the wave propagation) reaches 90° (*i.e.*, where the longitudinal field component goes to zero and then reverses). Several studies have provided evidence for such polarization inversion (Kundu *et al.*, 1977; Webb *et al.*, 1983; Alissandrakis and Kundu, 1982, 1984; Brosius *et al.*, 1992; Schmelz *et al.*, 1992).

The observations made by Gopalswamy, White, and Kundu (1991) and White, Thejappa, and Kundu (1992) showed that the SVC polarization changes its sign at high frequencies (near 5 GHz), according to the mode coupling theory, but the frequency of the change of the polarization sign is often inconsistent with the theoretical estimates. Gopalswamy *et al.* (1994) showed that this difficulty could be eliminated if we consider the propagation of radio waves through a plasma current layer. A similar difficulty was also noted by Schmelz *et al.* (1992). They used magnetic properties of the QT layer to extrapolate the magnetic field to the corona above an active region to determine the plasma density in the layers.

In May 1991, high-resolution Very Large Array (VLA) radio maps of active regions were constructed at three frequencies: 4.9, 8.4, and 15 GHz. The comparison of these data with magnetograms of active regions showed that the inversion and depolarization occur in different places of an active region, depending on the change of frequency (Lee *et al.*, 1996). Tokhchukova and Bogod (2003) showed that in flare-producing active regions a more complex phenomenon is observed: Before an intense flare the sign of polarization changes twice when the frequency varies within a narrow interval.

Radio observations of the polarized radiation indicate that flare-producing active regions (FPARs) display rather complex structure of the magnetic field already at early stages of the pre-flare phase. Since the polarized radio emission above sunspots at centimeter wavelengths is generated at the base of the corona and in the upper part of the transition layer from the chromosphere to the corona, the radio observations provide a direct method of detection of coronal magnetic fields at these heights, which are difficult to reach at X-ray and UV wavelengths. In the study by Bogod and Tokhchukova (2006) specific features of radio emission occurring before and during a flare are marked. These are particularly seen at centimeter wavelengths in the form of an inhomogeneous structure displaying various frequency inversions of the circular polarization as single, double, and multiple changes of the sign of circular polarization. Here we present a few examples that occurred in flare-producing ARs of double inversions of polarization sign along a frequency.

The spectral and polarization observations of FPARs during the maximum of the 23rd cycle of solar activity provided new information about the fine spectral features in their radio emission. In particular, many peculiar features in the polarized emission were observed at microwave wavelengths with the multiwave spectrograph attached to the RATAN-600 radio telescope. The double and multiple polarization inversions are the most intriguing among them. The nature of the phenomena is related to the flare productivity of active regions, as it follows from the data presented here and in a previous study by Bogod and Tokhchukova (2003).

Here, we present samples of multifrequency observations of FPARs with RATAN-600 combined with data obtained by the Solar and Heliospheric Observatory (SOHO) and the Geostationary Operational Environmental Satellite (GOES) spacecraft. The frequency analysis of the observed inversion of the polarization in such FPARs has been carried out, and several versions of possible interpretation for the double polarization inversion have been developed, with estimates for their relative probability.

2. Description of RATAN-600 Observations

We use the regular observational mode of the RATAN-600 radio telescope. This telescope features a combination of an instantaneous frequency spectrum from 1 to 16 GHz (from which, in this study, we use the band from 4 to 16 GHz) with a frequency resolution of about 5% – 15% and high sensitivity in measuring small levels of circular polarization (about 0.05%) and radiation flux of several Jy (1 Jy = 10^{-26} Wm^{-2} Hz^{-1}). This sensitivity results from the wide band of receiver frequencies (600 – 800 MHz), the parallel analysis of the spectrum, and the large collection surface (600 – 1000 m^2). The RATAN-600 radio telescope has a moderate spatial resolution in the horizontal plane ($<$15 arcseconds at a wavelength 1.83 cm) and a low resolution in the vertical plane (approximately 15 arcminutes at the same wavelength). The diagram dimensions vary in proportion to wavelength.

2.1. The Time Interval 10 – 13 July 2000

Within the considered time interval the "Bastille Day" flare in NOAA AR 9077 occurred on 14 July 2000. Figure 1 presents simultaneous one-dimensional scans of the solar disk at several wavelengths from 3.83 to 6.52 cm. AR 9077 was situated in the northern hemisphere during the total considered time interval. To the West from AR 9077 two other active regions, NOAA 9069 and 9070, were seen on the disk; they displayed relatively stable polarization structure in the entire spectral band, with minor temporal variations (see Figure 1). NOAA 9077 was a flare-producing region. In X rays, it generated 3 X-class, 10 M-class, and 11 C-class flares.

We can see in Figure 1 that the structure of such FPARs displays sharp variations of polarized emission at wavelengths of 4.32, 4.62, and 4.93 cm in comparison with nonflare active regions NOAA 9069 and NOAA 9070. The middle panel of the figure presents the magnetic field structure (Michelson Doppler Imager data, SOHO/MDI), showing smaller day-to-day variations of complexity. From RATAN-600 detailed spectral and polarization observations at microwaves one can determine the frequency band in which the FPAR one-dimensional structure varied sharply. In Figure 1 it corresponds to wavelengths of 4.32, 4.62, and 4.93 cm. At these wavelengths, both for the entire radio source and for its parts, positive-to-negative and opposite inversions of the sign of polarization were detected. The flux spectra in intensity and circular polarization are presented in Figure 4.

2.2. The Time Interval 12 – 15 June 2004

Within this period AR NOAA 10634 was observed on the eastern limb (see Figure 2). According to Space Weather Highlight Bulletin 1502, this AR was isolated on the disk during the considered period of time. According to GOES data, AR NOAA 10634 produced an intense M-level flare and five C-level flares on 13 June, which we relate to the FPAR. Figure 2 presents the behavior of AR NOAA 10634 at different wavelengths. Shown are the 1-D RATAN-600 microwave observations of AR NOAA 10634 in Stokes parameters I (a) and V (b). The scans for different wavelengths from 2.24 to 6.52 cm are located from bottom to top.

As we can see from Figure 2b, only the radio structure of AR NOAA 10634 in polarized emission demonstrates a sharp nonmonotonic behavior. In contrast, two other ARs

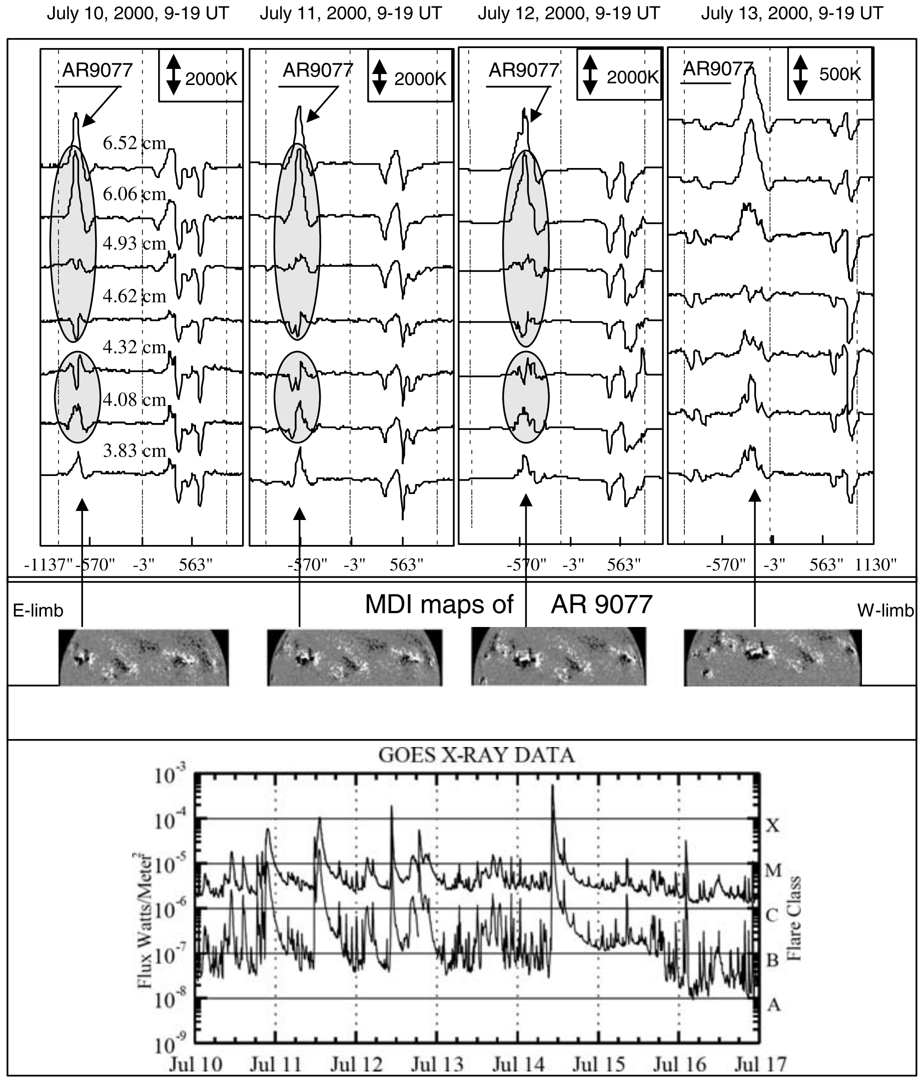

Figure 1 Solar disk scans at several centimeter wavelengths for the time of observations from 10 to 13 July 2000. Located in the eastern part of the scan is AR NOAA 9077, in which the intense "Bastille Day" flare occurred on 14 July. Located in the western hemisphere are two nonflare active regions, NOAA 9069 and NOAA 9070. The structure of AR NOAA 9077 demonstrates sharper changes in the structure of the polarized emission at wavelengths of 4.32, 4.62, and 4.93 cm, in comparison with the nonflare active regions (see also Tokhchukova and Bogod, 2003). The middle panel of the figure presents the magnetic field structure (SOHO/MDI data) indicating smaller variations of complexity. The soft X-ray flux indicating flare activity of AR NOAA 9077 (GOES data) is presented in the lower panel.

(10633 and 10632) located to the West from AR NOAA 10634 were stable and displayed the monotonic increase of polarized emission with wavelength.

It is interesting to note that the only for AR NOAA 10634 the polarization always changes sign at different wavelengths; for stable sources the polarization spectra is monotonic.

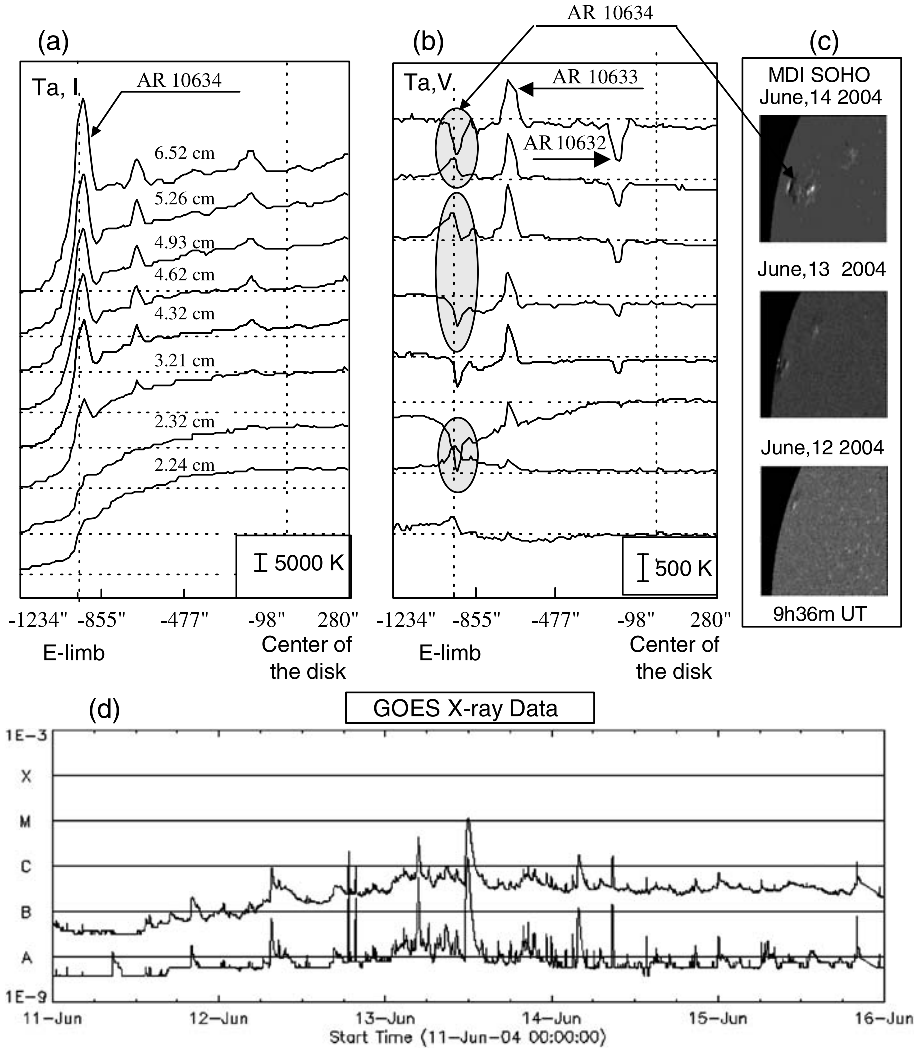

Figure 2 The structure of AR 10634 polarization at different wavelengths. RATAN-600 multiwave one-dimensional scans at different wavelengths made with the knife-beam diagram on 12 June 2004 in intensity (a) (T_a, I) and in polarized emission (b) (T_a, V). From the polarization curves one can see the multiple polarization inversions in the AR 10634 radiation. To the West, two stable sources associated with AR 10633 and 10632 are seen. Both active regions demonstrate monotonic behavior of the polarized emission along the spectrum. (c) The evolution of AR 10634 in MDI data. (d) The activity of AR 10634 at X-ray wavelengths. The most intense flare occurred on 13 June 2004.

Note also that, according to GOES-10 data, the activity in the X-ray range was dominated by AR 10634. The magnetic field maps (Figure 2c) present the evolution of AR 10634 from 12 to 14 June. The comparison between the data obtained with MDI and RATAN spectral polarization scans for the FPAR shows that the complex polarization structure of the AR is detected around 1 to 2 days before it can be seen in MDI data; since the active region is close to the limb, the line-of-sight magnetograms are not reliable sources of information. Thereby the radio data make it possible to determine the complex structure of the FPAR magnetic field earlier.

2.3. The Time Interval 5 – 8 March 2004

The spectral polarization analysis provides a very convenient tool to determine the activity of active regions appearing on the eastern limb. Since a radio source is located at some height above the photosphere, its radio image may be observed at different wavelengths and the level of its activity may be determined during one, two, or even three days before the time when the optical image of the magnetic field becomes available for analysis. Here, we present some observations of such type. Figure 3 presents the appearance of AR NOAA 10570 on the eastern limb from 5 to 8 March 2004. The two upper panels present the polarization of the radiation in the form of one-dimensional (1-D) scans at several wavelengths from 1.92 to 4.93 cm. For comparison, the SOHO/MDI map is shown below. The bottom panel shows the X-ray activity according to GOES data during the time interval 3 to 8 March 2004; since the events from 5 to 8 March come from AR 10570, we can identify this region as a FPAR. Seen on 5 March is a dramatic complication of the structure of the polarized emission of the radio source at wavelengths in the range 2.67 – 4.32 cm (marked by ellipses), which results in double reversal of the polarization sign along the frequency spectrum. The AR was not yet visible in SOHO/MDI data on this day; a distinct magnetic image appeared only on 6 or 7 March. In accordance with GOES data, the activity of AR NOAA 10570 at X-ray wavelengths accompanies the complicated behavior of its radio polarization spectrum. Later on, after 8 March, the radio polarization structure along the spectrum becomes stable, being accompanied with a decrease flare activity.

3. Analysis of Observations

Here, we will describe the peculiarity in the polarized radiation of FPARs in the form of double inversion of the polarization sign and will analyze possible reasons for the phenomenon.

Such irregular polarization structures coexist in the same scans with regular polarization structures, ruling out instrumental effects. For example, one can compare in Figure 1 the irregular polarization structure for AR 9077 (marked by an oval) and the regular polarization structure for AR 9069 and AR 9070. Another example is in Figure 2, if one compares the polarization structure of AR 10634 (marked by an oval) and that of AR 10632 and AR 10633.

We will analyze in more detail the observations of active region NOAA 9077, in which the “Bastille Day” flare occurred on 14 July 2000. As was previously noted, in this case, as well as in other presented observations, the double reversal of the polarization sign at the short-wavelength part of the microwave range was observed. Figure 4 presents the intensity and polarization spectra of AR NOAA 9077 for 13 July 2000.

Figure 5 presents the magnetic field reconstruction of this region from the paper by Yan (2003). It should be taken into account that the magnetic field displays a complicated multi-loop structure up to heights of about 40 arcseconds.

This configuration contains the magnetic loops that were involved in the eruption resulting from a catastrophic loss of mechanical balance between magnetic tension and pressure (Forbes, 2000; Amari *et al.*, 2000).

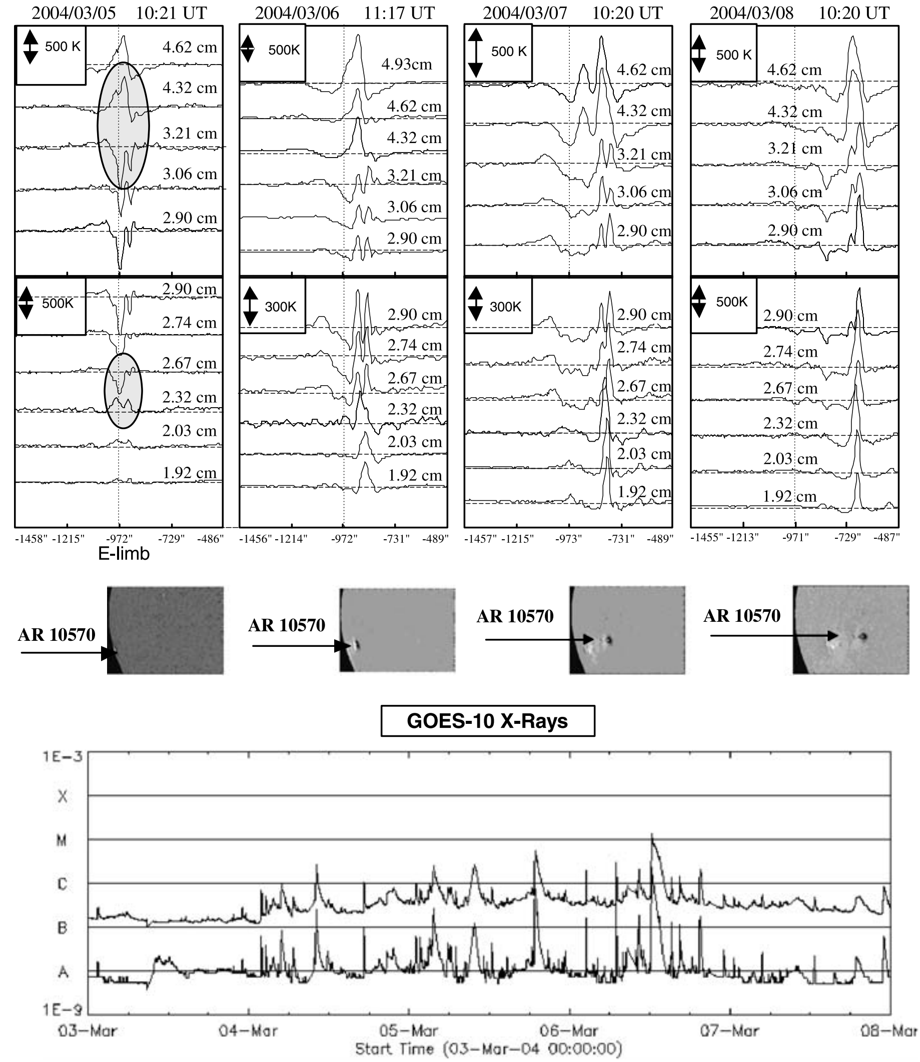

Figure 3 RATAN-600 one-dimensional scans of the Sun from 5 to 8 March 2004, at several wavelengths from 1.92 to 4.93 cm. Under the scans, the SOHO/MDI magnetic field maps are shown. The bottom panel gives the GOES X-ray data for the period 3 to 8 March 2004. One sees the day-to-day changes in the structure of AR NOAA 10570 in polarized radiation at microwaves, accompanied by a decrease of its flare activity. There was one more active region, NOAA 10567, located in the western hemisphere (beyond the figure frame), that was stable and showed a monotonic growth of the microwave spectrum with wavelength.

Figure 6 presents a detailed comparison of the circular polarization structure of the active region NOAA 9077 at the neighboring wavelengths of 4.08 and 4.62 cm along with the magnetic field for 13 July from SOHO/MDI. The dramatic change of the polarization sign is seen in the central part of the active region, above the magnetic neutral line. As follows from a comparison of Figures 5 and 6, the region of the reversal of the polarization sign occurs in the eastern part of the magnetic rope, where the core of the Bastille Day Flare occurred. This example shows that the change of the polarization sign can occur in active

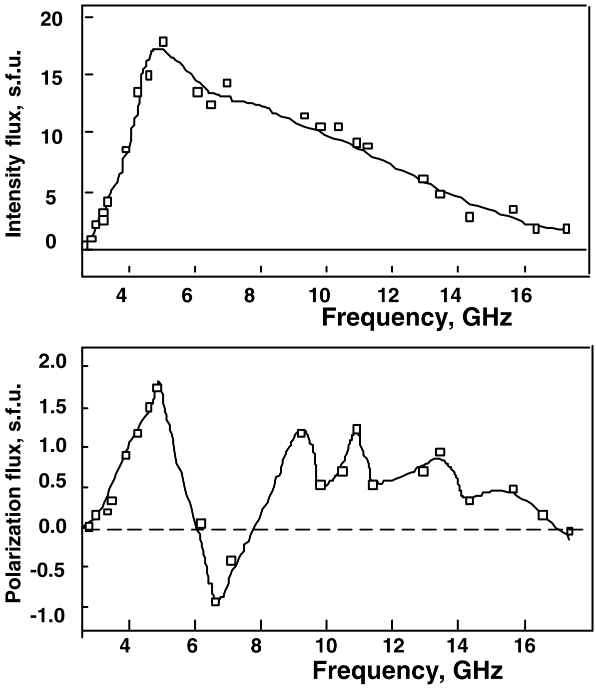

Figure 4 The intensity and polarization spectra (*I* and *V* Stokes parameters) of active region NOAA 9077 for 13 July 2000, displaying a double reversal of the polarization sign.

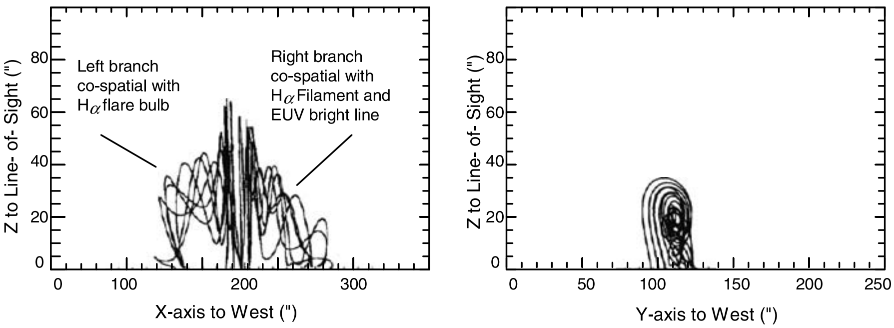

Figure 5 The structure of the magnetic field lines in active region NOAA 9077, reproduced from Yan (2003). The abscissa corresponds to the distance along the Sun surface; the ordinate plots the height (both in arcseconds).

regions with a complex magnetic field structure, which have a double inversion of magnetic field direction in relation to the observer. In the following we shall consider this and other possible reasons for the change of the polarization sign.

3.1. The Nature of the Depolarization of the Microwave Emission

Let us analyze possible reasons for the depolarization of the microwave emission, which occurs in the form of the double inversion, and estimate the physical parameters of the regions in which such inversion may occur.

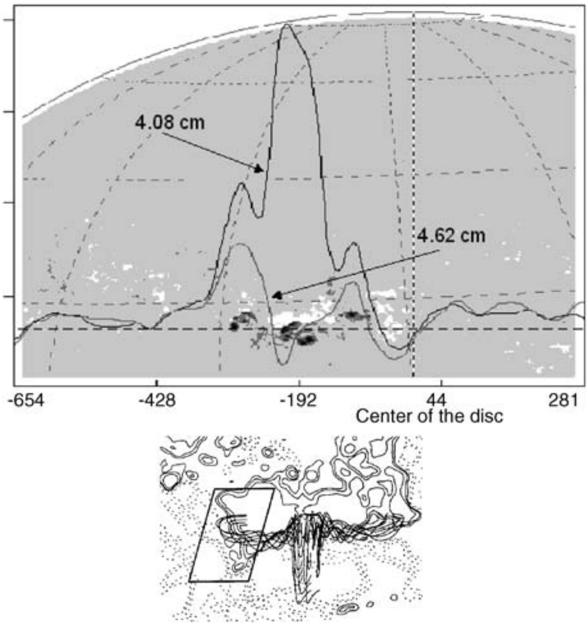

Figure 6 Top: Comparison of the circular polarization structure of the active region NOAA 9077 at the neighboring radio wavelengths 4.08 and 4.62 cm with its magnetic structure observed by SOHO MDI on 13 July 2000 shown overlaid. Bottom: Comparison with the reconstructed magnetic rope superimposed on the Huairow magnetogram (courtesy of Y. Yan). The rhombus marks the location of the core of the "Bastille Day" flare that occurred on the next day. The left circular polarization is directed upward and the right one directed downward.

3.1.1. Polarization Inversion due to the Propagation of Radio Emission through QT Magnetic Field Regions

The double inversion of the polarization sign occurs within a relatively narrow band width of about 15% – 20%. It is known that, in the approximation of geometrical optics, the ordinary and extraordinary waves propagate through inhomogeneous solar plasma independently. When this approximation is violated, the waves become linearly coupled. In particular, when one type of wave falls onto the coupling region, waves of both types result. Interaction of different types of waves is possible for QT propagation within a region both with divergent magnetic field and with zero magnetic field.

The coupling strength depends on the coupling parameters in the regions indicated. For example, for the region of QT propagation with divergent magnetic field this parameter depends on the inhomogeneity of the magnetic field orientation (Cohen, 1960; Zheleznyakov, 1970),

$$G_{\perp} = \frac{\omega_{\mathrm{p}}^2 \omega_{\mathrm{B}}^3}{c\omega^4 |\mathrm{d}\alpha/\mathrm{d}z|}, \tag{1}$$

where ω_{p} is the plasma frequency, ω_{B} is the gyrofrequency, and α is the angle between the line of sight and the direction of the magnetic force lines.

In this situation, the sign of polarization should reverse at the frequencies at which $G_{\perp} \approx 1$ in both regions of QT propagation. From Equation (1) it follows that these regions should have similar values of magnetic field strength. Since the value of $G_{\perp}$ depends on the magnetic field strength more than on the electron density, we can estimate B. For example, for $n_{\mathrm{e}} = 10^9$ cm^{-3} and frequency $f = 6.5 \times 10^9$ Hz the magnetic field strength is $B = 40$ G.

The frequency range of the region of the polarization inversion is basically determined by the variation of the magnetic field in the regions of QT propagation. From observations on 11 – 13 July 2000 (see Figure 4) it follows that the polarization inversion occurs in the band

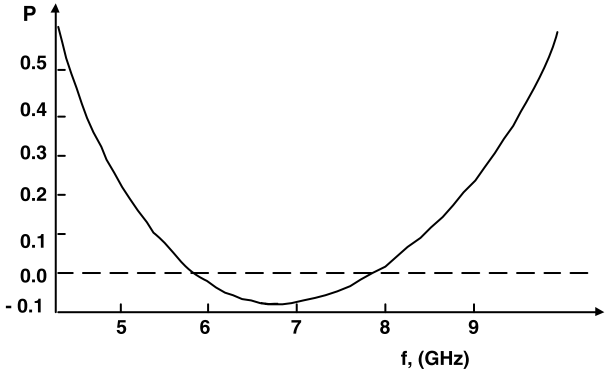

Figure 7 The polarization degree p as a function of frequency f for the case of two regions of the QT magnetic field.

$\Delta f \approx 0.2f = 1.5 \times 10^9$ Hz. From Equation (1) and Figure 4 it follows that for a constant electron density in the second QT region the magnetic field $B \cong 30$ G. At low frequencies, the wave mode remains the same, but the sign of rotation of the electric vector will reverse twice, in accordance with the orientation of the magnetic field. At high frequencies, $G_\perp < 1$ and the sign of the electric vector rotation will not vary. The degree of circular polarization will vary according to (Zheleznyakov, 1977)

$$p = 1 - 2\exp\bigl[-2\delta_0(\omega_{\mathrm{B}})\bigr], \tag{2}$$

where

$$\delta_0(\omega_{\mathrm{B}}) \cong \frac{\pi\omega_{\mathrm{p}}^2\omega_{\mathrm{B}}^3}{16c\omega^4|\mathrm{d}\alpha/\mathrm{d}z|}.$$

For the passage of two QT layers, the degree of circular polarization can be determined as follows:

$$p = \bigl\{1 - 2\exp\bigl[-2\delta_0(\omega_{\mathrm{B}})\bigr]\bigr\}\bigl\{1 - 2\exp\bigl[-2\delta_0(\omega_{\mathrm{B}} - \Delta\omega_{\mathrm{B}})\bigr]\bigr\}, \tag{3}$$

where $\omega_{\mathrm{B}} - \Delta\omega_{\mathrm{B}}$ is the gyrofrequency in the second higher layer of QT propagation.

Taking into account Figure 4, the dependence of the polarization degree on frequency is shown in Figure 7.

We can see from Figure 7 that the polarization curve is qualitatively consistent with the observations on 13 July 2000 (Figure 4), but the negative degree of polarization reaches only 0.1 whereas near 7 GHz the degree of polarization is equal to 0.9.

3.1.2. The Inversion of Polarization due to the Propagation of Radio Emission through Regions with Zero Magnetic Field

Radio wave propagation through a zero magnetic field region is possible, if, for example, a current sheet is along the way. Such a situation is quite probable in flare-productive active regions. In this case, the characteristic parameter of the coupling is equal to (Zheleznyakov, 1970)

$$G_0 = 8\sqrt{2}\frac{\omega_{\mathrm{p}}^2|\cos^3\alpha|}{c|\mathrm{d}\omega_{\mathrm{B}}/\mathrm{d}z|}. \tag{4}$$

Strong coupling occurs at $G_0 \ll 1$. Note that this parameter substantially depends on the angle and is independent of the frequency. Strong coupling occurs only at angles $\alpha \approx \pi/2$. At angles $\alpha \neq \pi/2$, $G_0 \gg 1$ and the approximation of geometrical optics also remains valid for the propagation of waves through the neutral current sheet. Thereby, in this case the observed inversion of the sign of polarization could occur, if the current sheet is approximately parallel to the solar surface.

It is plausible that the radiation at different frequencies occurs at different heights, and even for a comparatively simple spherical current sheet, which follow, for example, the spherical surface of the photosphere. Radio waves with different frequencies can propagate at different angles to the surface of the current sheet. This fact may result in the change of the polarization sign in a narrow frequency range, since the angular dependence of G_0 is rather strong. In this case, a double change of the polarization sign will be observed, since at the edges of the frequency band the condition $\alpha \neq \pi/2$ is fulfilled and the sign of the polarization will be the same.

For simplicity, let us consider a model of a vertical magnetic dipole located at depth $d = 10^4$ km under the photosphere and a magnetic field strength at the photosphere of $B_0 =$ 2500 G (Takakura, 1972). The field varies with height as

$$B(h) = \frac{B_0}{(1 + h/d)^3}\ [\mathrm{G}]. \tag{5}$$

This formula makes it possible to determine the height of the third gyroresonance level h. Numerous studies show that the most intense radiation may be emitted from this level (*e.g.*, White, Kundu, and Gopalswamy, 1991; Nindos *et al.*, 2000). Figure 8 presents the schematic layout of a current sheet above the Sun; here, $R_\oplus$ is the solar radius, h_0 is the height of the radio source at the frequency where the parameter V reaches its minimum, and h is the height at which the polarization inversion occurs. Above the source, the current sheet is located at some distance r (see Figure 8). If we know the angular distance of the active region from the central meridian ϕ, the curvature radius r of the current sheet can be determined for $h - h_0 \ll r$ as

$$r = \frac{(h - h_0)\sin\phi}{\cos\alpha_{\mathrm{cr}}}, \tag{6}$$

where α_{cr} is the angle of crossing the current sheet by radio waves at which $G_0 = 1$.

It is generally accepted that the magnetic field at the edges of the current sheet is roughly equal to 100 G, the thickness of the sheet is equal to 100 cm (Syrovatskii, 1976; Heyvaerts and Priest, 1976; Heyvaerts, Priest, and Rust, 1977), and $n_{\mathrm{e}} = 10^9\ \mathrm{cm}^{-3}$. If, for example, in agreement with Figure 4, h corresponds to a frequency of 6.2 GHz, h_0 corresponds to a frequency of 7 GHz, and $h(f)$ is determined by Equation (5) then $r = 3.1 \times 10^8 \sin(\phi) \leq 3.1 \times 10^8$ cm. From this relation it follows that, to preserve the spectrum near the polarization inversion frequency with time (and thereby with the angle) that is observed, r should depend on ϕ. This condition is hardly fulfilled on the Sun. The long-term existence of neutral current sheets is unlikely, owing to the tearing instability. The current sheet may be stable in the presence of a weak magnetic field orthogonal to the neutral current plane (Schindler, 1974). The condition of instability suppression is specified in the following way:

$$\upsilon_T/\omega_{\mathrm{B,c}} < \sqrt{\upsilon_{\mathrm{T}} L/\omega_{\mathrm{B,e}}},$$

where υ_{T} is the thermal velocity of electrons, $\omega_{\mathrm{B,c}}$ is the gyrofrequency in the center of the current sheet, $\omega_{\mathrm{B,e}}$ is the gyrofrequency at the edges of the current sheet, and L is the thickness of the current sheet.

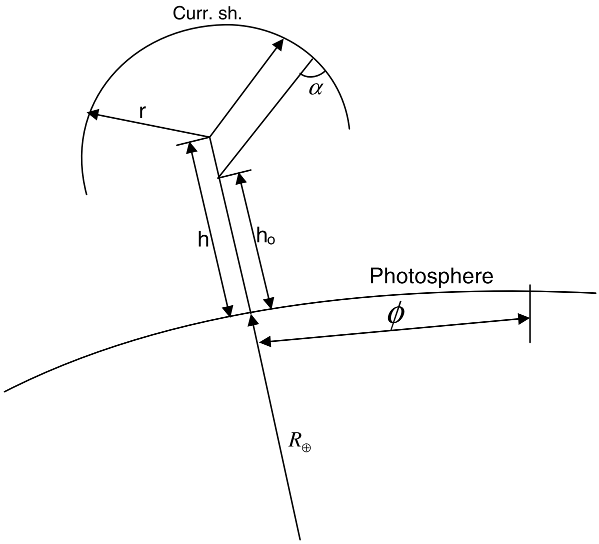

Figure 8 The propagation of a radio wave through the current sheet. $R_\oplus$ is the radius of the Sun, h_0 is the height of the radio source at the frequency at which the parameter V reaches its minimum, and h is the height at which the polarization inversion occurs. The current sheet is located above the source at a distance h with curvature r. The angle ϕ is the angular distance of the active region from the central meridian.

The stabilization occurs at the level of $\omega_{\mathrm{B,c}}/\omega_{\mathrm{B,e}} = 0.1 - 0.03$ if the magnetic field outside the sheet is $B_\mathrm{e} = 10 - 100$ G, the electron temperature is $T_\mathrm{e} = 10^6$ K, and the thickness of the sheet is $L = 100$ cm (Syrovatskii, 1976; Heyvaerts and Priest, 1976; Heyvaerts, Priest, and Rust, 1977).

In such a sheet, because of the structure of the magnetic field, QT propagation takes place along a wide range of angles (Zheleznyakov, Kocharovsky, and Kocharovsky, 1996). Correspondingly, the range of angles in which strong coupling takes place also expands:

$$\tan^{5/4}\alpha > \tan^{5/4}\alpha_{\mathrm{cr}} = \frac{\omega_{\mathrm{B,c}}}{\omega_{\mathrm{B,e}}}\left(\frac{\sqrt{2}c\omega^4}{\omega_\mathrm{p}^2\omega_{\mathrm{B,e}}^3 L}\right)^{1/4}.$$

In this case, the change of the polarization sign will occur if, as above, the radiation at different frequencies crosses the current sheet at different angles. At the polarization inversion frequency, the radiation should be emitted at an angle $\alpha < \alpha_{\mathrm{cr}}$. If the parameters of the current sheet are the same as above, and if, for example, $n_\mathrm{e} = 10^9\ \mathrm{cm}^{-3}$, then at a frequency near 7 GHz and for $B_\mathrm{e} = 10 - 100$ G the interval of critical angles will be within $\alpha_{\mathrm{cr}} = 89.8^\circ - 87.2^\circ$. Therefore, a strong interaction will occur if the radiation propagates virtually parallel to the current sheet. If the current sheet is located above the radio source, the polarization inversion is possible at the frequencies at which the radiation crosses the current sheet when the position of the source varies depending on the frequency. The excessive number of parameters makes it difficult to construct an unambiguous model in this case, but some conclusions can be reached as follows. A thin sheet should be essentially parallel to the line of sight (*i.e.*, closer to vertical). The length of a current sheet should be small so that the radiation can cross it only within a narrow interval of frequencies. The size of the current sheet and the source should be about the same, so that the inversion of the polarization becomes more essential. The shape of a thin sheet should be close to planar. However, as in the previous models, it is hard to expect that a constant frequency interval of the inversion of the polarization sign will be observed when the source changes its position on the solar disk with the passage of time. The projection of the current sheet on the radiating loop will vary and so will the frequency interval of the inversion of the sign of polarization. Therefore, the observed pattern of the inversion of the polarization sign may be a result of the linear coupling of waves in the region of a zero QT magnetic field, but strict conditions are required to restrict the geometry of this region.

3.1.3. Polarization Inversion due to the Propagation of Radio Emission through Turbulent Regions in the Plasma

Another possible reason for the change of the polarization sign can be the scattering of electromagnetic waves on waves of plasma turbulence (Ledenev *et al.*, 2002). In this case, the intensities of the ordinary (o) and extraordinary waves (x) in the passage of a layer with the plasma turbulence will vary according to the expressions

$$\begin{aligned} I_{\mathrm{x}}(\omega,\tau) &= I_{\mathrm{xo}}\exp\bigl\{-\tau/\cos(\theta)\bigl[1+f_2(\omega)/f_1(\omega)\cos(\theta)\bigr]\bigr\},\\ I_{\mathrm{o}}(\omega,\tau) &= I_{\mathrm{oo}}\exp\bigl\{-\tau/\cos(\theta)\bigl[1-f_2(\omega)/f_1(\omega)\cos(\theta)\bigr]\bigr\}, \end{aligned} \tag{7}$$

where

$$\begin{aligned} f_1(\omega) &= \bigl\{\bigl[(\omega-\omega_{\mathrm{p}})^2-\omega_{\mathrm{p}}^2\bigr]^{1/2}+\bigl[\bigl(\omega+\omega_{\mathrm{p}}^2\bigr)^2-\omega_{\mathrm{p}}^2\bigr]^{1/2}\bigr\}/2\omega,\\ f_2(\omega) &= \bigl\{\bigl[\omega_{\mathrm{B}}(\omega+\omega_{\mathrm{p}})^{-1}+\omega_{\mathrm{B}}/\omega\bigr]\bigl[(\omega+\omega_{\mathrm{p}})^2-\omega_{\mathrm{p}}^2\bigr]^{1/2}\\ &\quad+\bigl[\omega_{\mathrm{B}}(\omega-\omega_p)^{-1}+\omega_{\mathrm{B}}/\omega\bigr]\bigl[(\omega-\omega_{\mathrm{B}})^2-\omega_{\mathrm{p}}^2\bigr]^{1/2}\bigr\}/2\omega. \end{aligned}$$

Here $\tau=\sigma f_1(\omega)L/\upsilon_{\mathrm{gr}}\equiv\tau_0 f_1(\omega)$ is the optical thickness due to scattering in a region with thickness L, υ_{gr} is the group velocity of electromagnetic waves,

$$\sigma=\frac{\pi}{3}\frac{\omega_{\mathrm{p}}^2}{\upsilon_{\mathrm{gr}}}\frac{kT}{mc^2}\frac{W}{n_{\mathrm{e}}T}\frac{1}{k_{1\max}-k_{1\min}},$$

W is the energy of Langmuir turbulence in units of volume, $k_{1\max}$ and $k_{1\min}$ are the maximum and minimum wave number of Langmuir turbulence, respectively, I_{xo} and I_{oo} are the intensities of ordinary and extraordinary waves falling onto the scattered layer, and θ is the angle between the line of sight and a normal line to the layer. From relation (7), we can obtain for the polarization degree

$$p(\omega,\tau)=\frac{I_{\mathrm{x}}(\omega,\tau)-I_{\mathrm{o}}(\omega,\tau)}{I_{\mathrm{x}}(\omega,\tau)+I_{\mathrm{o}}(\omega,\tau)}=\frac{I_{\mathrm{xo}}-I_{\mathrm{oo}}\exp[2\tau_{\mathrm{o}}\cdot f_2(\omega)]}{I_{\mathrm{xo}}+I_{\mathrm{oo}}\exp[2\tau_{\mathrm{o}}\cdot f_2(\omega)]}.$$

The extraordinary wave is subjected to greater scattering and, therefore, its greater weakening may result in the change of the polarization sign. Note that the intensity of the extraordinary wave radiation should decrease essentially because of the scattering. We will present some calculations for this mechanism, assuming that $\omega_{\mathrm{p}}=7\times10^9$ Hz, $\omega_{\mathrm{B}}=0.3\omega_{\mathrm{p}}$, $I_{\mathrm{xo}}=1$, $I_{\mathrm{oo}}=0.1$, and $\tau_{\mathrm{o}}=10$. Then the degree of polarization will vary monotonically from -0.7 at a frequency of 3×10^9 Hz to 0.4 at a frequency of 9×10^9 Hz. The degree of polarization will indeed change its sign at a wavelength close to 4.5 cm as observed (see Figure 9). The problem is that the required optical thickness should be large (since at smaller τ, the variation of the degree of polarization essentially decreases, which is not consistent with observations), which implies the necessity of a high level of plasma turbulence in the scattering region. Such turbulence should result in increased radiation at the frequency $2\omega_{\mathrm{p}}$ (*i.e.*, at $\lambda\approx13.5$ cm), which is not confirmed by our observations.

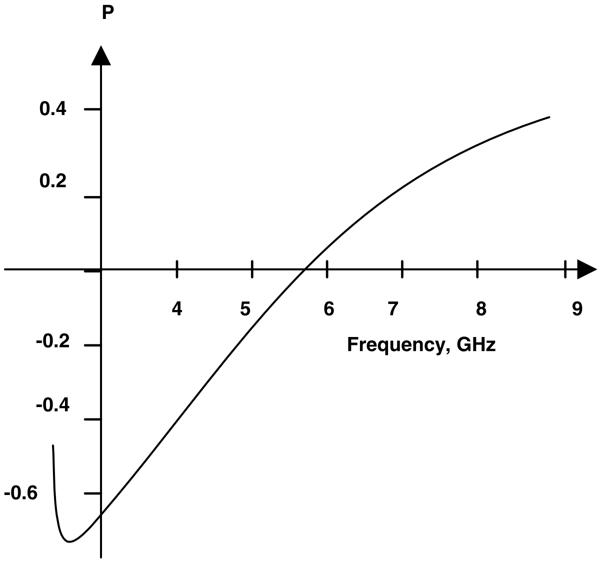

Figure 9 Change of the polarization degree resulting from scattering of electromagnetic waves by plasma waves.

3.1.4. The Inversion of Polarization due to the Propagation of Radio Emission through a Prominence Region

An active region can contain a cold filament. We carried out detailed calculations of the radio emission of an active region with a cold filament located in the atmosphere specified by the model by Zlotnik (1968), which is consistent with the average spectral characteristics of the radio emission from active regions. It turned out that the presence of a cold filament (or, more exactly, a region with reduced electron temperature) does not result in the change of the polarization sign. This is related to the fact that the optical thickness of gyroresonance levels is proportional to T_e^{s-1} for $s \geq 2$, where s is the harmonic number.

At low temperatures, obtaining an optical thickness that exceeds unity for the extraordinary wave at the third gyroresonance level requires a high electron plasma density. However, at such density the fourth gyroresonance level also starts to radiate with sufficient efficiency owing to its high temperature.

The presence of a cold filament in the environment with a constant temperature (for example, in the corona) itself results in excessive o-mode radiation, although no change of the polarization sign occurs, since beyond the filament the degree of polarization is equal to zero. Calculations made using the model with a filament, which is hot relative to the surrounding plasma, show that in this case the change of the polarization sign may be simply obtained. This conclusion does not depend on the location of this filament.

Figure 10 presents an example of the calculation of the Stokes parameter V as a function of frequency. A hot filament with a temperature of 5×10^5 K is located in the transition region at heights from 7500 to 8000 km. The height of the lower boundary of the corona was supposed to be 9000 km, and the height of the chromosphere was 4000 km. The magnetic field was specified by Equation (5).

In this model of the magnetic field, the thickness of the hot filament should not exceed 10^8 cm. Only in this case will a change of the polarization sign occur in 20% of the frequency band. In this interval, such a change should be accompanied by a substantial increase of the intensity of the radiation. This will result in the occurrence of narrow cyclotron lines, which

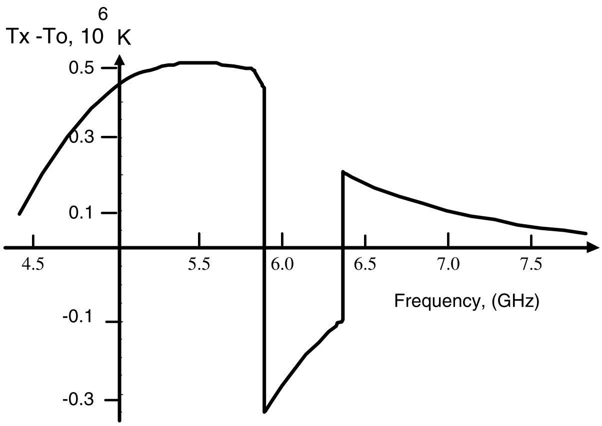

Figure 10 The frequency dependence of the Stokes parameter V for the model with a warm filament.

were discussed in detail in the study by Zheleznyakov and Zlotnik (1980). In this model, the intensity of the cyclotron lines exceeds the intensity of the radiation in the adjacent frequency regions almost by an order of the magnitude. These observational data show that this increase (if any) occurs in a lower frequency range. Thereby, this reason for the change of the polarization sign also displays substantial drawbacks.

3.1.5. The Inversion of Polarization due to the Propagation of Radio Emission through Regions with Complex Magnetic Fields

Another possible cause for polarization inversion may be the change of the direction of the magnetic field in the regions of effective radiation at different frequencies. Such a topology may occur in complex magnetic field structures, an example of which is presented in Figure 11. For example, when the third gyroresonance level moves onto the slope of such a magnetic "dip," owing to the change in the direction of the magnetic field the sign of the rotation of the extraordinary wave relative to the observer will coincide with that of the o-mode wave at the second gyroresonance level beyond the "dip," which may result in the polarization inversion.

If we assume that the dependence of the magnetic field strength along the magnetic field line is described by Equation (5) and the change of the polarization sign occurs in 20% of the frequency band in the vicinity of wavelengths of $4-5$ cm, then the size of the "dip" in the front plane should be about 1.2×10^8 cm. Note that in this case the Stokes parameter I should not undergo essential variations with frequency, which is consistent with our observations. In this model, a weak dependence of the frequency interval of the polarization inversion on the displacement of the active region across the solar disk also occurs. When radio waves propagate above this structure of the magnetic field, they will inevitably cross the region of QT magnetic field; the polarization sign will be conserved provided it is the region of isotropic propagation of radio waves. The condition of isotropic propagation, at which the sign of rotation of an electromagnetic wave remains constant when the direction of the magnetic field along the line of sight varies, follows from Equation (1) for $G_\perp \ll 1$:

$$B < \frac{\omega^{4/3}}{7.8 \times 10^6} \left(\frac{|\mathrm{d}\alpha/\mathrm{d}z|}{n_\mathrm{e}} \right)^{1/3}.$$

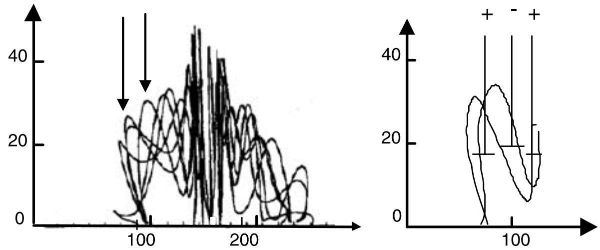

Figure 11 The layout of the propagation of the extraordinary (or ordinary) wave in the presence of deflection by magnetic lines. Left: Copy of Figure 5, with arrows indicating the magnetic field lines drawn on the right side of the figure. Symbols + and – denote different signs of wave rotation. Both coordinate axes are in arcseconds.

When α varies from 10° to 45° at a distance of about 10^9 cm and n_e varies within 10^8 – 10^9 cm^{-3}, the isotropic propagation of radio waves at wavelengths of 4 – 5 cm occurs for $B < 10 – 30$ G. Thereby, the magnetic rope, in which magnetic lines are deflected, should be surrounded by a magnetic field with $B < 10 – 30$ G. The gyroresonance level that corresponds to the third harmonic of the gyrofrequency at $\lambda = 4.5$ cm displays a magnetic field of about 700 G. Thus, to conserve the sign of the polarization, the deflection of the magnetic field should be maintained within the interval $B = 700$ G to $B = 10 – 30$ G. This condition apparently substantially constrains the model for the double reversal of the polarization sign.

3.1.6. The Inversion of Polarization due to the Propagation of Radio Emission through a High Electron Density Region

Another possibility for the double change of the polarization sign may be related to the propagation of radio waves through a region of increased electron plasma density. The frequency at which the refraction index for the extraordinary wave is equal to zero is

$$\omega_{\mathrm{cr}} = \frac{1}{2}\left(\omega_{\mathrm{B}} + \sqrt{\omega_{\mathrm{B}}^2 + 4\omega_{\mathrm{p}}^2}\right).$$

The frequency for which the refraction index for the ordinary wave is equal to zero is $\omega = \omega_{\mathrm{p}}$.

If the region of radiation (the most effectively x-mode radiating gyroresonance layer) is located below the region with increased electron density, then at the frequencies $\omega > \omega_{\mathrm{cr}}$ the polarization sign corresponds to the extraordinary wave, whereas at the frequencies $\omega_{\mathrm{p}} < \omega < \omega_{\mathrm{cr}}$ it corresponds to the ordinary wave. Therefore, at high frequencies the polarization sign will correspond to the x-mode wave. With a decrease of frequency within an interval, the condition will be fulfilled. Then, if the most efficiently radiating gyroresonance layer at the x-mode wave is lower than the region with increased electron density, the sign of polarization will correspond to the ordinary wave. With a further decrease of the frequency, the efficiently radiating gyroresonance layer at the x-mode wave may be located above the region with increased electron density, and then the sign of polarization will again correspond to that of the x-mode wave. For example, let the frequency of the polarization inversion be close to 6.5×10^9 Hz, then the density in the center of the region with increased electron density should be within the interval $3.3 \times 10^{11} \leq n_e \leq 5.2 \times 10^{11}$ cm^{-3}. In this case, at the indicated frequency the x-mode wave will not be able to propagate through the region with increased electron density, in contrast to the o-mode wave. It is clear that such an electron density in active regions at the heights of efficient centimeter-wave radiation may be reached either in dense filaments or current sheets. The high density in a current sheet is directly related to the condition $2n_e kT = B^2/8\pi$, where T is the temperature in the sheet and B is the magnetic induction in the vicinity of the sheet. As a rule, equilibrium temperatures do not exceed 10^5 K (Syrovatskii, 1976; Heyvaerts and Priest, 1976). Thus, if $B = 10$ G then $n_e > 10^{11}$ cm^{-3}.

According to different estimates, the sheet thickness may reach several tens of centimeters (Syrovatskii, 1976; Heyvaerts, Priest, and Rust, 1977), which results in the small contribution of the current sheet to the Stokes parameter I. The temperature in a hot current sheet, which may be formed if either the ion-cyclotron or ion-sound turbulence is established in it (Farafonov and Charikov, 1983), may reach $(1-2) \times 10^7$ K while the electron density is about $5.5n_e$, where n_e is the electron density of the plasma surrounding the current sheet. It is obvious that in this case it is difficult to expect a change of the polarization sign at short-wavelength microwaves.

However, the model with the current sheet suggests only a single change of the polarization sign, since even with the decrease of the frequency the effectively radiating gyroresonance layer at the x-mode wave will be located above the region of increased electron density and the polarization sense will correspond to the x-mode wave. Still, because of reversal of the direction of the magnetic field at the other side of the current sheet, the direction of rotation of the electric vector in the wave will remain the same.

4. Conclusion

We will briefly summarize the aspects of each of the suggested mechanisms that result in the double reversal of the sign of polarization of the microwave radiation of active regions. All of them are connected with complex magnetic fields in active regions, which, in principle, are present in flare-productive active regions, such as for example NOAA 9077.

1. The linear coupling of waves in the region of quasitransverse magnetic field cannot yield any appreciable variation of the polarization sign in a narrow frequency range.
2. Unrealistic constraints on the geometry of the region of zero magnetic field are required for the linear coupling of waves in the region of zero magnetic field.
3. A current sheet stabilized by a weak magnetic field, orthogonal to the sheet surface, is more favorable for the interpretation of the observed change of the polarization sign. However, in this case it is difficult to obtain the observed constancy of the frequency interval in the inversion of the polarization sign as the position of the source on the solar disk varies.
4. For scattering of radio waves by waves of high-frequency plasma turbulence, a substantial variation of the polarization sign occurs only for a high level of the turbulence, which should also produce considerable radiation at long wavelengths. No such radiation is observed in the investigated active regions.
5. The presence of a cold filament does not result in the double change of the polarization sign. In the case of a model with a hot filament, it is easy to obtain the observed double change of the polarization sign; however, this case should result in the occurrence of so-called cyclotron lines, which is not consistent with the observations presented.
6. Another possibility for the double inversion of the polarization sign may be related to passing of waves through a region of increased electron density. However, if the region of increased electron density is a current sheet there will be only a single change of the

polarization sign and if such region is a filament then a too high density ($3.3 \times 10^{11} \leq n_e \leq 5.2 \times 10^{11}$ cm^{-3}) is required.

7. The presence of magnetic "dips" or a magnetic rope, in which the direction of the magnetic field lines can change sign relative to the observer at distances of about 1000 – 2000 km, well explains all the observed characteristics. In this model, the frequency range of the polarization inversion effect as the active region crosses the solar disk is invariant. This is also consistent with observations. Such structure of the magnetic field should be essentially isolated. Otherwise, the polarization sign will correspond to the direction of the magnetic field in the region of transition from nonisotropic to isotropic propagation of radio waves and it can change the spectrum of the polarized radiation in the frequency range where the polarization sign reverses. Calculations show that the radiating region thus should be surrounded by a magnetic field with $B < 10 - 40$ G.

Thus all the double inversion mechanisms under our consideration have their own singularities. In our opinion the model with magnetic "dips" agrees better with the observations than most of the others.

Acknowledgements We thank the anonymous reviewer, whose careful corrections to the article have contributed to its improvement. This research was supported by grants 09-02-00111 and 08-02-00378 of RFBR of Russia and OFN-15 program of Russian academy of Sciences.

References

Alissandrakis, C.E., Kundu, M.R.: 1982, *Astrophys. J.* **253**, L49.
Alissandrakis, C.E., Kundu, M.R.: 1984, *Astron. Astrophys.* **139**, 271.
Amari, T., Luciani, J.F., Mikic, Z., Linker, J.: 2000, *Astrophys. J.* **529**, L49.
Bandiera, R.: 1982, *Astron. Astrophys.* **112**, 52.
Bogod, V.M., Tochchukova, S.K.: 2003, *Astron. Lett.* **29**(4), 263.
Bogod, V.M., Tokhchukova, S.K.: 2006, *Cosmic Res.* **44**(6), 506.
Brosius, J.W., Willson, R.F., Holman, G.D., Schmelz, J.T.: 1992, *Astrophys. J.* **386**, 347.
Cohen, M.H.: 1960, *Astrophys. J.* **131**, 664.
Farafonov, V.G., Charikov, J.E.: 1983, *Soln. Dannye* **12**, 96.
Forbes, T.G.: 2000, *Phil. Trans. Roy. Soc. Lond.* **358**, 771.
Gopalswamy, N., White, S.M., Kundu, M.R.: 1991, *Astrophys. J.* **379**, 366.
Gopalswamy, N., Zheleznyakov, V.V., White, S.M., Kundu, M.R.: 1994, *Solar Phys.* **155**, 339.
Heyvaerts, J., Priest, E.R.: 1976, *Solar Phys.* **47**, 223.
Heyvaerts, J., Priest, E.R., Rust, D.M.: 1977, *Astrophys. J.* **216**, 123.
Kundu, M.R., Alissandrakis, C.E., Bregman, J.D., Hin, A.C.: 1977, *Astrophys. J.* **213**, 278.
Ledenev, V.G., Tirsky, V.V., Tomozov, V.M., Zlobec, P.: 2002, *Astron. Astrophys.* **392**, 1089.
Lee, J., White, S., Gopalswamy, N., Kundu, M.R.: 1996, *Bull. Am. Astron. Soc.* **28**, 873.
Nindos, A., Kundu, M.R., White, S.M., Shibasaki, K., Gopalswamy, N.: 2000, *Astrophys. J. Suppl.* **130**, 485.
Peterova, N.G., Akhmedov, S.B.: 1974, *Sov. Astron.* **17**, 168.
Piddington, J.H., Minnett, H.C.: 1951, *Aust. J. Sci. Res. A* **4**, 131.
Schindler, K.J.: 1974, *J. Geophys. Res.* **79**, 2803.
Schmelz, J.T., Holman, G.D., Brosius, J.W., Gonzalez, R.D.: 1992, *Astrophys. J.* **399**, 733.
Syrovatskii, S.I.: 1976, *Pis'ma Astron. Zh.* **2**, 35.
Takakura, T.: 1972, *Solar Phys.* **26**, 151.
Tokhchukova, S.K., Bogod, V.M.: 2003, *Astron. Lett.* **212**, 99.
Webb, D.F., Davis, J.M., Kundu, M.R., Velusamy, T.: 1983, *Solar Phys.* **85**, 267.
White, S.M., Thejappa, G., Kundu, M.R.: 1992, *Solar Phys.* **138**, 163.
White, S.M., Kundu, M.R., Gopalswamy, N.: 1991, *Astrophys. J.* **366**, L43.
Yan, Y.: 2003, *Space Sci. Rev.* **107**(1), 119.
Zheleznyakov, V.V.: 1970, *Radio Emission of the Sun and Planets*, Pergamon, Oxford. ed. J.S. Hey.

Zheleznyakov, V.V.: 1977, *Electromagnetic Waves in Space Plasma: Generation and Propagation*, Nauka, Moscow, 432. In Russian.
Zheleznyakov, V.V., Zlotnik, E.Y.: 1980, In: Kundu, M.R., Gergely, T.E. (eds.) *Radio Physics of the Sun*, *IAU Symp.* **86**, Reidel, Dordrecht, 87.
Zheleznyakov, V.V., Kocharovsky, V.V., Kocharovsky, V.V.: 1996, *Astron. Astrophys.* **306**, 685.
Zlotnik, E.Y.: 1968, *Sov. Astron.* **12**, 245.